日本 *AEM* 学会誌 *Vol. 6, No. 2 (1998)*

学術論文

Principle of Sensor Elimination in Interior Permanent Magnet Motors

Mengesha Mamo
Jun OYAMA Member
Takashi ABE Member
Tsuyoshi HIGUCHI Member
Eiji Yamada Member

In this paper we present a high frequency method of sensor elimination in interior permanent magnet motor drives. Characteristics of the carrier frequency component voltage (CFCV), from Pulse Width Modulation (PWM) inverters, and the corresponding Carrier Frequency Component Current (CFCC) are studied and used as the rotor position information source. Mathematical expression relating the rotor position to the CFCV, CFCC and the motor parameters are developed and simplified. It is shown by simulation that the rotor position can be calculated from measured values of CFCV and CFCC at appropriately selected instants.

Key Words: CFCV, CFCC, assumed rotor position, actual rotor position

1 Introduction

The problem of sensor elimination in permanent magnet motors have been attracting the attention of many researchers due to the high efficiency and torque density of permanent magnet motors. Interior Permanent Magnet (IPM) motors have relatively high inductance than the Surface Permanent Magnet (SPM), and can be used for wider field weakening operation. The q-component inductance is larger than the d-component inductance and hence, can generate reluctance torque. Elimination of rotor position sensor enhances the torque density, increases the reliability and reduce the overall cost of the drive [2]. Many authors have reported on sensor elimination methods [2]-[6]. Most of the reported sensor elimination methods are, directly or indirectly, based on estimation of the rotor position from counter EMF. The counter EMF method is typically valied above 10 % base speed, because of the difficulty in estimating the counter EMF at low speed. Reference [6] proposed a current injection method for the speed range from zero to 10 % base speed. In this range the rotor position angle is obtained from the detected voltages induced by adding sine wave slight currents. The requirement for additional slight AC current and the possible torque disturbance due to the slight AC current are drawbacks of this method.

In this paper the rotor position of an IPM motor is related to the Carrier Frequency Component Voltage (CFCV) of the PWM-inverter, the corresponding Carrier Frequency Component Current (CFCC) and the motor parameters. The rotor position from this relation is independent of the rotor speed for high carrier frequency. There is neither AC current source requirement for injection nor torque disturbance. In addition to this introduction this paper has five sections. In section 2 the scheme of the proposed sensor elimination method is presented. In section 3 math-

Corespondence : Mengesha Mamo, Nagasaki University, 1-14 Bunkyo-Machi, Nagasaki-852, Japan

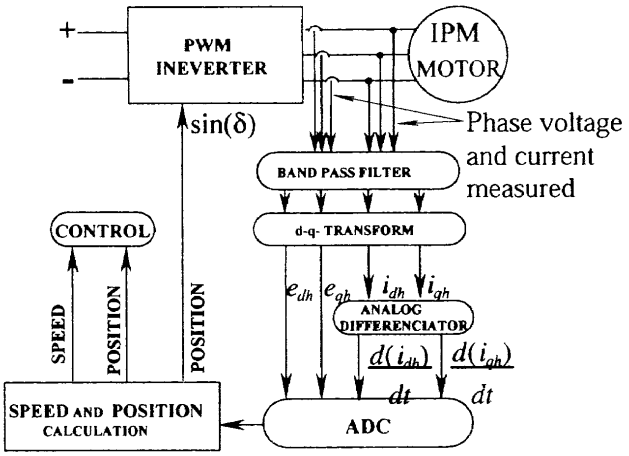

Fig. 1: Scheme of the rotor position determination

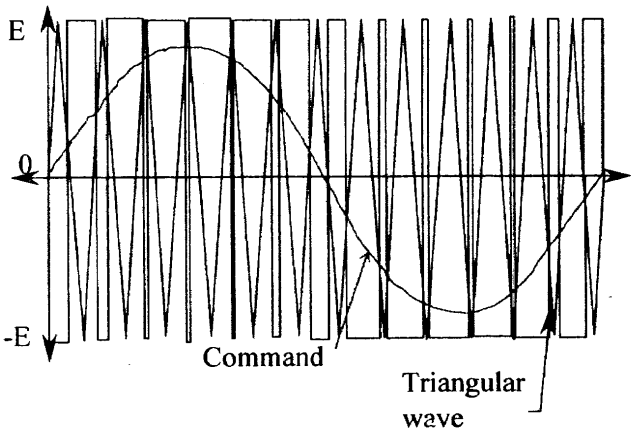

(a) Switching pattern of a PWM inverter.

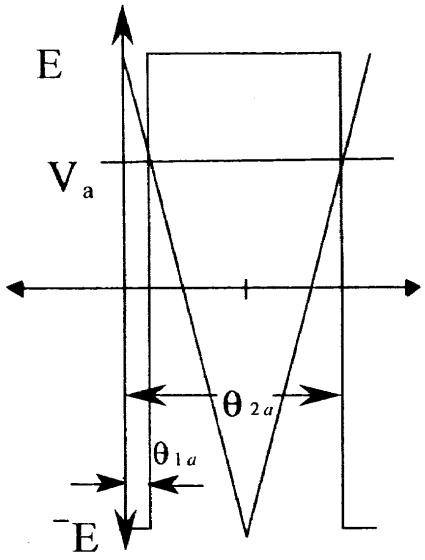

(b) Pulse form in one switching style

Fig. 2: Switching schemes with a triangular reference wave

ematical expression is derived for the CFCV. In section 4 the coordinate axes corresponding to the actual rotor position and the assumed rotor position are explained. In section 5 the CFCV and CFCC resolved at the assumed rotor position are related to the rotor position. The rotor position calculated from these relations are presented and discussed. The last section is conclusion.

2 Scheme of The Rotor Position Determination

The CFCV and CFCC in the three phases of motor terminal are measured and transformed to d-q components at an assumed rotor position, as shown in Fig. 1. The current is differentiated with respect to time. The d-q voltage and the differentiated d-q current are converted to digital signal to be processed by a microprocessor. The rotor position and speed can be output for control and switching.

3 Carrier Frequency Component Voltage

Output pulse of a voltage-source PWM inverter with the switching triangular wave and the command voltage are shown in Fig. 2 (a). It can be seen that pulse form of Fig. 2 (b) is repeating

at the triangular wave frequency called the carrier frequency. This pulse form is between two consecutive triangular wave peaks and is varying in width. We can express this varying width, θ_{1a} and θ_{2a}, in terms of the command voltage and the dc voltage as in equation (1a) and equation (1b) [1]. Once the pulse width is expressed as a function of the command voltage and the dc voltage, we can apply Fourier series expansion to Fig.1 (b) considering its periodicity.

$$\theta_{1a} = \frac{\pi}{2}(1 - \frac{\nu_{1a}}{E}) \tag{1a}$$

$$\theta_{2a} = \frac{\pi}{2}(3 + \frac{\nu_{1a}}{E}) \tag{1b}$$

$$\begin{aligned} e_a &= -E \quad 0 \le \omega_c t \le \theta_{1a} \\ e_a &= E \quad \theta_{1a}\omega_c t \le \theta_{2a} \\ e_a &= -E \quad \theta_{2a} \le \omega_c t \le \pi \end{aligned} \tag{2}$$

Where, E = dc voltage,

ν_{1a}= command voltage ω_c= carrier frequency in radians per second.

The Fourier series expansion cosine term of CFCV fundamental component coefficient, E_{ah} can be calculated to be as in equation (3).

$$E_{ah} - \frac{1}{2\pi}\int_0^{2\pi} e_a \cos(\theta)d\theta$$

$$= -\frac{2}{\pi}E\cos(\frac{\pi\nu_a}{2E}) \tag{3}$$

The sine term is found to be zero.

Hence, the CFCV cosine term for phase-a, E_{ah}, can be expressed as in equation (4).

$$e_{ah} = -\frac{2}{\pi}E\cos(\frac{\pi\nu_a}{2E})\cos(\omega_c t) \tag{4}$$

We can rewrite equation (4) as a sine function, equation (4a), by shifting the origin of the coordinate axis $\pi/2$ to the left, along the $\omega_c t$-axis.

$$e_{ah} = -\frac{2}{\pi}E\cos(\frac{\pi\nu_a}{2E})\sin(\omega_c t) \tag{4a}$$

Similar approach for phase-b and phase-c CFCV results in equations (4b) and (4c).

$$e_{bh} = -\frac{2}{\pi}E\cos(\frac{\pi\nu_b}{2E}\sin(\omega_c t + \alpha) \tag{4b}$$

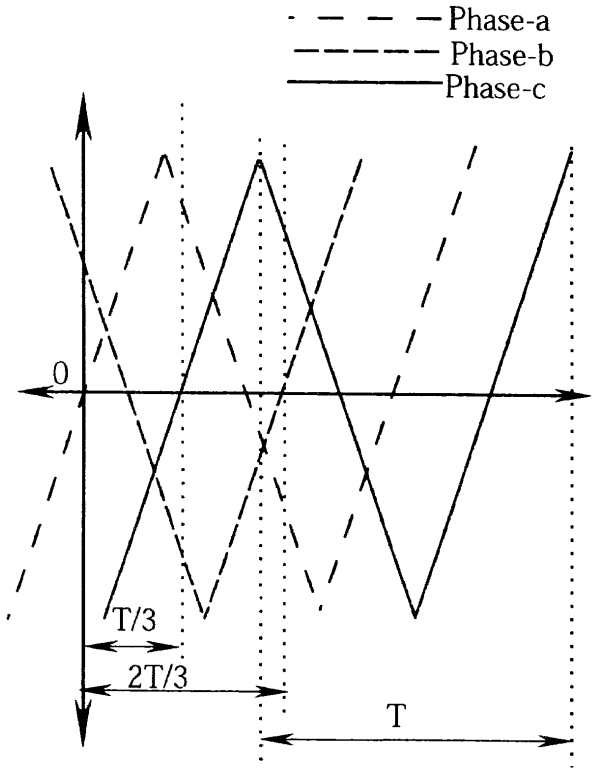

Fig. 3: Triangular wave for the three phases with T/3 (period) phase difference

$$e_{ch} = -\frac{2}{\pi}E\cos(\frac{\pi\nu_c}{2E})\sin(\omega_c t + \beta) \tag{4c}$$

The value of α an β in equations (4b) and (4c) depends on the triangular wave used for generating the PWM. If the same triangular wave is used in all the three phases both α and β are zero. Hence, the CFCV in the three phases are in phase. On the other hand if the triangular wave used in the three phases are different and have some phase difference, which vary with command frequency, it can be shown that α and β are functions of the carrier frequency to command frequency ratio [1]. Let us consider one period of the triangular wave to be T (sec), and the three phases have T/3 (sec.) time shift irrespective of command frequency, as shown in Fig.3. In this case the carrier frequency component voltage in the three phases become 120 degrees out of phase. Hence, equations (4b) and (4c) can be modified as in equations (5a) and (5b).

$$e_{bh} = -\frac{2}{\pi}E\cos(\frac{\pi\nu_b}{2E})\sin(\omega_c t - 120) \tag{5a}$$

$$e_{ch} = -\frac{2}{\pi} E \cos(\frac{\pi \nu_c}{2E}) \sin(\omega_c t + 120) \qquad (5b)$$

4 Characteristics of The CFCV

The CFCV is inversely amplitude modulated by the command voltage. That is, the CFCV amplitude varies between the maximum and minimum two times in a command frequency cycle, where the minimum amplitude of the CFCV is at the maximum of the command frequency amplitude and vice versa. The minimum amplitude depends on the command voltage peak to dc voltage ratio. It is zero and the CFCV becomes discontinuous if the ratio is greater or equal to one. The CFCV is simulated for carrier frequency of 2 kHz, command frequency of 50 Hz, dc voltage of 100 volts and command voltage peak of 50 volts in Fig. 4 and 5. The command voltage peak to dc voltage ratio is 1/2 in Fig. 4, this is usually the case in PWM inverters. The minimum amplitude is more than 60% of the maximum amplitude as can be observed in Fig. 4. Hence, the variation in the amplitude of the CFCV in one switching cycle can be neglected. The peak amplitude of the CFCV is about 60% of dc voltage. The first four cycles of CFCV in phase-a, -b and -c is shown in Fig. 5. As can be seen the CFCV in the three phases are 120 degrees out of phase and have some amplitude difference since their corresponding command voltage are at different instantaneous values.

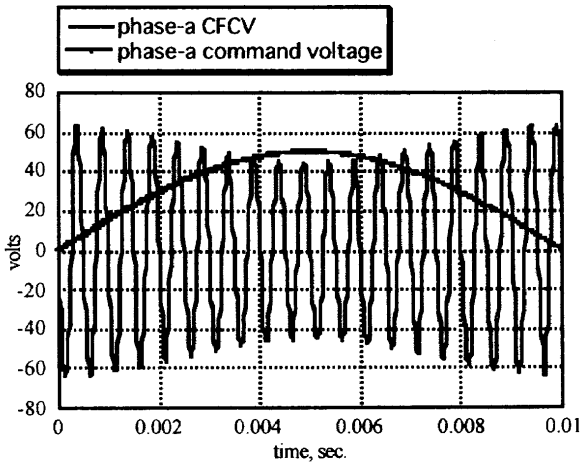

Fig. 4: Phase-a CFCV and command voltage in half command frequency cycle.

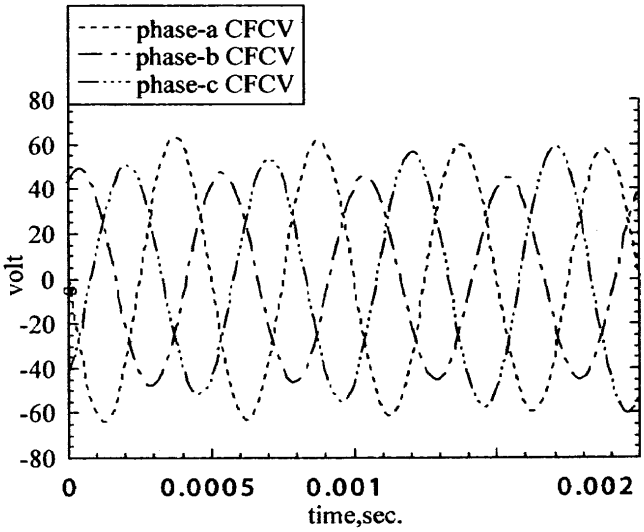

Fig. 5: CFCV in phase-a, -b, and -c are120 degrees (electrical) out of phase.

5 Relation of The CFCV to The Rotor Position

IPM synchronous motors are characterized by the fact that the phase inductance varies appreciably as a function of the rotor position [2]. That is, IPM synchronous motor inductance variation is similar to that of a salient pole synchronous motor with the d- and q-axis inductance reversed. Hence, its magnetic circuit can be represented as a salient pole synchronous motor with the d-axis corresponding to the q-axis of the salient pole synchronous motor [3].

5.1 Two Coordinate Axes

We can include the rotor position in a two quadrature resolved CFCV equation by considering two coordinate axes, as shown in Fig. 6 [1]. The first coordinate axis corresponds to an assumed rotor position, where the d-axis is θ degrees from the axis of phase-a, while the other coordinate axis corresponds to the actual rotor position. The d- axis of the actual rotor position corresponds to the north pole of the permanent

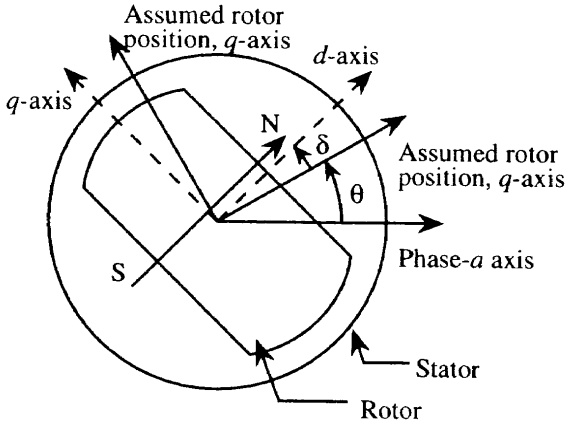

Fig. 6: Two coordinate axes and an IPM as a salient synchronous motor

magnet on the rotor. The voltage and current are transformed to d - q components at the assumed rotor position, equations (6a) and (6b).

$$e_{dh} = \{\frac{3}{2}L_{aao} + L_{al} - \frac{3}{2}L_{g2}\cos(2\delta)\}\frac{di_{dh}}{dt} + \frac{3}{2}L_{g2}\sin(2\delta)\frac{di_{qh}}{dt} \quad (6a)$$

$$e_{qh} = \{\frac{3}{2}L_{aao} + L_{al} + \frac{3}{2}L_{g2}\cos(2\delta)\}\frac{di_{qh}}{dt} + \frac{3}{2}L_{g2}\sin(2\delta)\frac{di_{dh}}{dt} \quad (6b)$$

5.2 *Mathematical Expression for Rotor Position*

We can solve equations (6a) and (6b) simultaneously for $\sin(2\delta)$ and $\cos(2\delta)$ and express as in equations (7a) and (7b).

$$\cos(2\delta) = \frac{e_{qh}\frac{di_{qh}}{dt} - e_{dh}\frac{di_{dh}}{dt} + \frac{(L_q+L_d)}{2}\{(\frac{di_{qh}}{dt})^2 - (\frac{di_{dh}}{dt})^2\}}{\frac{(L_q-L_d)}{2}\{(\frac{di_{dh}}{dt})^2 + (\frac{di_{qh}}{dt})^2\}} \quad (7a)$$

$$\sin(2\delta) = \frac{e_{dh}\frac{di_{qh}}{dt} + e_{qh}\frac{di_{dh}}{dt} - (L_q + L_d)\frac{di_{qh}}{dt}\frac{di_{dh}}{dt}}{\frac{(L_q-L_d)}{2}\{(\frac{di_{dh}}{dt})^2 + (\frac{di_{qh}}{dt})^2\}} \quad (7b)$$

Where L_d and L_q are the $d-q$ inductance of the motor, related to phase inductance by equations (7) and (8) in [3]. Hence, the rotor position can be calculated from equations (7a) and (7b). By using look-up tables $\sin(\delta)$ can be obtained. Calculation of equations (7a) and (7b) is to be done on-line. Common microprocessors may not be fast enough for on-line calculation of these equations. In the next subsection simplification of these equations is considered.

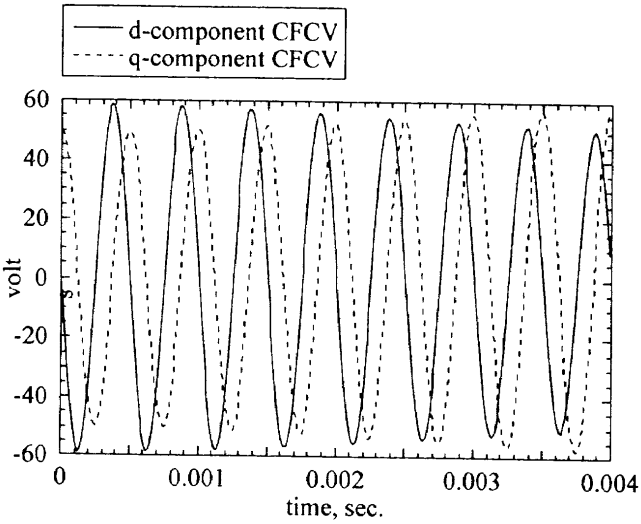

Fig. 7: d-q component CFCV have 90 degrees phase difference.

5.3 *Modification and Simplification of the Rotor Position Equation*

If three triangular waves are used in the PWM generation, as described in section 4, the CFCV resolved in to two coordinate components are 90 degrees out of phase, as shown on Fig. 7. The same is true for $\frac{di_{qh}}{dt}$ and $\frac{di_{dh}}{dt}$. Since the position of the rotor is required at most once per carrier frequency period, we can simplify equations (7a) and (7b) by choosing the instant $\frac{di_{qh}}{dt}$ or $\frac{di_{qh}}{dt}$ is zero.

$$\cos(2\delta) = \frac{e_{qh}}{\frac{(L_q+L_d)}{2}\frac{di_{qh}}{dt}} + \frac{L_q + L_d}{L_q - L_d} \quad (8a)$$

$$\sin(2\delta) = \frac{e_{dh}}{\frac{(L_q-L_d)}{2}\frac{di_{qh}}{dt}} \quad (8b)$$

Equations (8a) and (8b) are simplified equations at the instant $\frac{di_{dh}}{dt}$ is zero.

5.4 *Simulation*

Fig. 8 shows the flowchart of the simulation process. Fig. 9 and Fig. 10 show $\cos(2\delta)$,

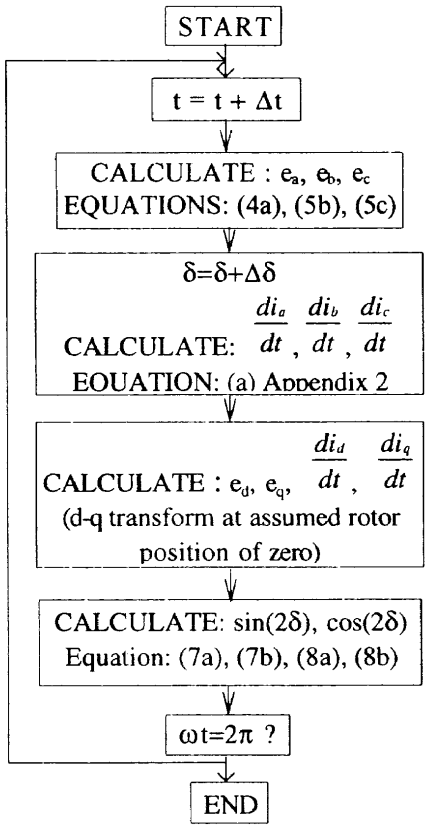

Fig. 8: Flowchart of simulation

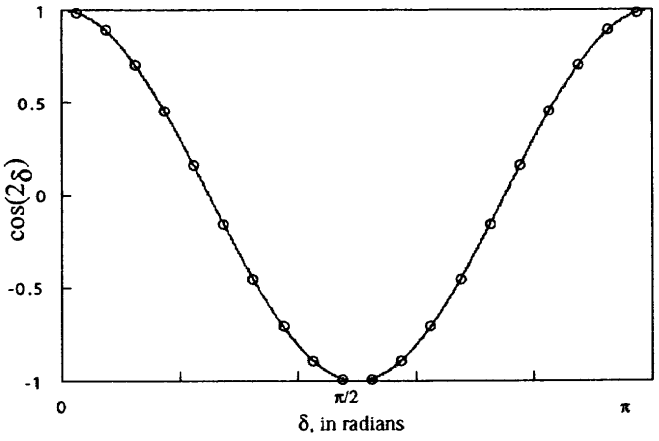

Fig. 9: $\cos(2\delta)$ from equation (8a) in half motor electrical cycle

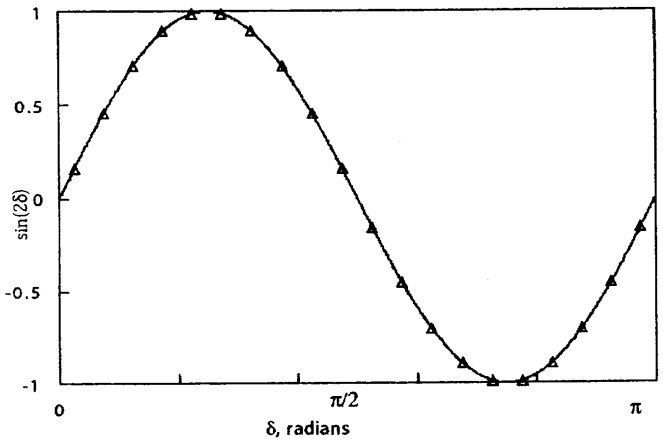

Fig. 10: $\sin(2\delta)$ from equation (8b) in half motor electrical cycle

and $\sin(2\delta)$ from equations (7a), (7b), (8a) and (8b). Equations (8a) and (8b) are calculated for the value of $\frac{di_{dh}}{dt}$ equal to zero. Hence, the rotor position available at any time is the position that corresponds to the last zero crossing of the $\frac{di_{dh}}{dt}$. Otherwise the rotor position at the point of calculation coincides with that of equations (7a) and (7b). The position error between two zero crossing of $\frac{di_{dh}}{dt}$ can be minimized by increased carrier frequency. The motor and inverter parameters used for the simulation are given in Appendix 1.

6 Conclusion

Expression is derived for the CFCV in a PWM inverter. It is shown by simulation that the rotor position can be calculated from the expression derived in terms of the CFCV, CFCC and motor parameters. The expression is simplified so that it gives rotor positions at appropriately

selected time intervals. The expression is so simple that it can be calculated by general propose microprocessors.

(1997 年 8 月 6 日受付)

Appendix

IPM motor parameters and ratings:
Rated power: 0.75 kW
Rated voltage: 100 volts
Rated speed: 1000 RPM
Ld :10 mH, (direct component inductance).
Lq :27 mH, (quadrature component inductance).
PWM inverter condition:
Carrier frequency : 2 kHz
Switching device: IGBT

Appendix 2

The general permanent magnet motor voltage equation[2]

$$\begin{bmatrix} e_a \\ e_b \\ e_c \end{bmatrix} - \begin{bmatrix} R & 0 & 0 \\ 0 & R & 0 \\ 0 & 0 & R \end{bmatrix} \begin{bmatrix} i_a \\ i_b \\ i_b \end{bmatrix} = \begin{bmatrix} L_{aa} & L_{ab} & L_{ac} \\ L_{ba} & L_{bb} & L_{bc} \\ L_{ca} & L_{cb} & L_{cc} \end{bmatrix} \frac{d}{dt} \begin{bmatrix} i_a \\ i_b \\ i_b \end{bmatrix}$$

$$+\frac{d}{dt} \begin{bmatrix} L_{aa} & L_{ab} & L_{ac} \\ L_{ba} & L_{bb} & L_{bc} \\ L_{ca} & L_{cb} & L_{cc} \end{bmatrix} \begin{bmatrix} i_a \\ i_b \\ i_c \end{bmatrix} + \frac{d}{dt} \begin{bmatrix} \lambda_m(\theta) \\ \lambda_m(\theta - 2\pi/3) \\ \lambda_m(\theta + 2\pi/3) \end{bmatrix} \quad \text{(a)}$$

$$L_{aa} = L_{aao} + L_{al} + L_{g2}\cos(2\theta) \quad \text{(aa)}$$

$$L_{bb} = L_{aao} + L_{al} + L_{g2}\cos(2\theta + 120°) \quad \text{(ab)}$$

$$L_{cc} = L_{aao} + L_{al} + L_{g2}\cos(2\theta - 120°) \quad \text{(ac)}$$

$$L_{ab} = L_{ba} = -\frac{1}{2}L_{aao} + L_{g2}\cos(2\theta - 120°) \quad \text{(ad)}$$

$$L_{bc} = L_{cb} = -\frac{1}{2}L_{aao} + L_{g2}\cos(2\theta) \quad \text{(ae)}$$

$$L_{ac} = L_{ca} = -\frac{1}{2}L_{aao} + L_{g2}\cos(2\theta + 120°) \quad \text{(af)}$$

Modified voltage equation for high frequency supply (e_{ah}, e_{bh}, e_{ch}),

$$\begin{bmatrix} e_{ah} \\ e_{bh} \\ e_{ch} \end{bmatrix} = \begin{bmatrix} L_{aa} & L_{ab} & L_{ac} \\ L_{ba} & L_{bb} & L_{bc} \\ L_{ca} & L_{cd} & L_{cc} \end{bmatrix} \frac{d}{dt} \begin{bmatrix} i_{ah} \\ i_{bh} \\ i_{ch} \end{bmatrix} \quad \text{(b)}$$

References

[1] Jun Oyama, Mengesha Mamo, Takashi Abe, Tsuyoshi Higuchi and Eiji Yamada, Sensor Elimination In Interior Permanent Magnet (IPM) Drives Using High Frequency Component Voltage From PWM-Inverter JIAS Conference, 1996.vol.3, pp E18-E23

[2] Nesimi Ertugrul and Poul A Nnew, Algorithm For Sensorless Operation Of Permanent Magnet Motors , IEEE Trans. Industry Applications, 1994, vol.30, No. 1., pp 126-133

[3] Ashok B. Kulkarni, and Mehrdad Ehsani A Novel Position Sensor Elimination Technique For The Interior Permanent Magnet Synchronous Motor Drive IEEE Trans. Ind. Applications, 1992, vol.28, No. 1., pp 144-150

[4] Rusong Wu and Gordon R.Slemon, "A Permanemt Magnet Motor Drive With out a Shaft Sensor", IEEE Trans. Ind. Applications, 1991, vol.27, No.5, pp 1005-1011

[5] Thomas M. Jahns, Gerald B. Kliman, and Thomas W. Neumann "Interior Permanent-Magnet Synchronous Motors for Adjustable-Speed Drives" IEEE Trans. Ind. Applications, 1986, vol.IA-22, No.4 , pp 738-747

[6] Nobuyuki Kasa and Hiroshi Watanabe, "For Practical Use Position and Speed Sensorless Salient-Pole Brushless DC Motor Drives" Proceedings of the Power Conversion Conference (PCC- NAGAOKA) , 1997, vol. 1, pp 127-132